

Bipolaron lattice formation at metal-polymer interfaces

P. S. Davids

Materials Science and Technology Division, Los Alamos National Laboratory, Los Alamos, New Mexico 87545

A. Saxena

Theoretical Division, Los Alamos National Laboratory, Los Alamos, New Mexico 87545

D. L. Smith

Materials Science and Technology Division, Los Alamos National Laboratory, Los Alamos, New Mexico 87545

(Received 13 July 1995)

We describe a model for metal-polymer interfaces based on the nondegenerate continuum model of Brazovskii and Kirova for the electronic properties of polymers. The correct analytic equations for a bipolaron lattice in this model are stated and the electronic properties of the bulk polymer, i.e., the energy-level structure, the energy density, and the chemical potential as a function of electron density are obtained numerically. We find that the bipolaron lattice is unstable at high densities when the intrinsic gap parameter exceeds a critical fraction of the total energy gap. The electronic properties of the bulk polymer are used for modeling the metal-polymer interface. The charge density near a metal-polymer interface is found from the electrostatic potential and an analytic expression for the bipolaron chemical potential assuming that the contact is in equilibrium with the polymer layer. Poisson's equation is integrated to determine the electrostatic potential. We find that a large charge density is transferred into the polymer layer if the Fermi level of the metal contact is higher than the negative bipolaron formation energy per particle or lower than the positive bipolaron formation energy per particle. The transferred charge lies very close to the metal-polymer interface as a bipolaron lattice with charge density progressively decreasing away from the interface. The transferred charge gives rise to a region of rapid "band bending," pins the Fermi level, and establishes the effective Schottky energy barrier. Upon increasing the metal Fermi level above the bipolaron formation energy per particle, the effective Schottky barrier saturates at the energy difference between the polaron formation energy and the bipolaron formation energy per particle. The model results are useful in interpreting recent measurements of internal photoemission, device electroabsorption, and capacitance-voltage characteristics in polymer light-emitting diodes.

I. INTRODUCTION

Periodic superstructures of nonlinear excitations such as soliton, polaron, and bipolaron lattices have been studied within continuum models for both degenerate¹ and nondegenerate ground state polymers.² The nondegenerate models are relevant to most polymers under consideration for use in optoelectronic and electronic devices. Conjugated polymers with phenyl rings in their backbones, such as poly(phenylene vinylene) (PPV) and its derivatives, e.g., poly[2-methoxy,5-(2'-ethyl-hexyloxy)-1,4 phenylene vinylene] (MEH-PPV) show pronounced electroluminescence.^{3,4} These polymers are organic semiconductors with energy gaps that depend on the molecular structure of the polymer. Polymer light-emitting diodes (PLED's) that emit throughout the visible spectrum have been successfully fabricated, using PPV and its derivatives.³⁻⁸ It is important to understand the nature of the metal-polymer interface and charge transfer across it to enhance the efficiency of these devices. To this end, a quantitative knowledge of the nature, density, and distribution of charge at metal-polymer interfaces is important.

Charge transferred into a nondegenerate polymer creates polarons and bipolarons. In the nondegenerate continuum model, the energy per particle of two isolated polarons is greater than that of a bipolaron, so there is binding of iso-

lated polarons to form bipolarons. Also in this model, a repulsive elastic interaction between bipolarons leads to the formation of a periodic structure, the bipolaron lattice.⁹ At zero temperature, the bipolaron lattice is the stable state for excess charge in the nondegenerate continuum model. The bipolaron lattice solution was obtained by several authors in different forms for nondegenerate polymer models.¹⁰⁻¹⁵ In Ref. 10, the solution was derived using inverse spectral theory, while Refs. 11,12 used the infinite lattice sum or the Poisson summation technique. Reference 13 obtained the grand potential and then used a simple ansatz to derive the bipolaron lattice solution. In Ref. 14, the solution was obtained for chains of finite length with periodic boundary conditions. The set of equations for the bipolaron lattice solution given in Refs. 10,15 is convenient for numerical calculations. However, the analytical expressions that have been published^{10,15} for the bipolaron lattice in the nondegenerate continuum model contain typographical errors.

In this paper, we describe the metal-polymer interface based on the Brazovskii-Kirova (BK) nondegenerate continuum model for conjugated polymers. The principal excitations in this model are polarons and bipolarons. We consider the high density limit (at zero temperature) in which the bipolarons form a lattice, because of their elastic interactions. In a previous paper,¹⁶ we considered low density effects (at

finite temperature) in which the charged excitations only interact electrostatically. Brazovskii and Kirova have previously used the degenerate version of their model in the high density, zero temperature limit to discuss a metal-polymer interface using analytical methods.¹⁷ However, they only presented the energy-level profiles schematically and did not obtain the electronic energy-level structure numerically.

In our interface model, the energy of the metal Fermi level relative to the bipolaron formation energy per particle in the polymer determines the charge density near the contact. The region of the polymer near a contact is assumed to be in equilibrium with that contact. Charge is exchanged between the contact and the polymer by forming a bipolaron lattice if the metal Fermi level is above the negative bipolaron formation energy per particle or below the positive bipolaron formation energy per particle. The nondegenerate continuum model describes a single polymer chain and a linear charge density (e/cm) per chain is determined by the chemical potential. For MEH-PPV and other PPV derivatives, the polymer chains are aligned primarily in the interfacial plane of the metal-polymer contact.¹⁸ We input the experimentally determined two-dimensional density of polymer chains and treat the chains as noninteracting (except electrostatically) to determine the total charge density. The one-dimensional bipolaron lattice, described by the nondegenerate continuum model, is on each polymer chain and thus lies in the interfacial plane. The linear charge density on a polymer chain depends on the distance of that chain from the metal interface. The total charge density at a given distance from the interface is the product of the linear charge density in the polymer chain at that distance and the two-dimensional density of polymer chains (which is independent of position). The charge distribution of the bipolaron lattices in the polymer chains is compensated by an opposite screening charge in the metal contact. We determine the charge in the polymer, at any given position, using the electrostatic potential at that position, the relationship between the chemical potential of the bipolaron lattice and the linear charge density in each polymer chain, and the two-dimensional density of polymer chains. Poisson's equation is integrated self-consistently to determine the electrostatic potential as a function of position.

We find that a large negative charge density is transferred into the polymer if the chemical potential of a contact is higher in energy than the negative bipolaron formation energy per particle and a large positive charge density is transferred into the polymer if the chemical potential of a contact is lower in energy than the positive bipolaron formation energy per particle. The transferred charge remains close to the metal-polymer interface and is screened by a charge of the opposite sign in the metal. In these cases, the Fermi energy at the polymer surface is effectively pinned at the bipolaron formation energy, due to the transferred charge near the interface. If the chemical potential of a contact lies between the formation energy per particle of the two kinds of charged bipolarons, there is no charge transfer at the metal-polymer interface and the Fermi energy at the polymer surface is not pinned by charge transfer. This is the kind of behavior that has been recently observed at polymer-metal interfaces in electroabsorption and internal photoemission experiments.¹⁹

The paper is organized as follows. In Sec. II, we present a

brief review of the nondegenerate continuum model of Brazovskii and Kirova. The corrected equations for the bipolaron lattice solution to the model are stated, the algorithm used to compute the energy levels of a bulk polymer is discussed, and numerical results for a bulk polymer are presented. In Sec. III, we describe a single metal-polymer interface, numerical results found by integrating Poisson's equation coupled with the relation between the polymer chemical potential and charge density are presented. We then discuss a metal-polymer-metal structure, which is similar to a polymer LED device. We summarize our conclusions in Sec. IV. The mathematical details of the bipolaron lattice solution and the intermediate steps in the derivation of the corrected analytical expression for the total energy are included in an Appendix.

II. NONDEGENERATE CONTINUUM MODEL

We describe the polymer using the (zero temperature) nondegenerate continuum model of Brazovskii and Kirova.² In this model, the energy gap arises from two sources: an intrinsic contribution produced by the splitting between bonding and antibonding electronic orbitals of the basic (rigid) structure of the polymer, and a contribution from the interaction of the electrons with a symmetry breaking atomic distortion (Peierls effect). The first contribution is responsible for the band gap in conventional semiconductors and the second contribution is the same as that which produces the energy gap in a degenerate ground state polymer like trans-polyacetylene. The Hamiltonian is given by

$$H = \int dx \psi^\dagger(x) \{ -i\hbar v_F \sigma_3 \partial_x + [\Delta(x)(\sigma_1 + i\sigma_2)/2 + \text{H.c.}] \} \times \psi(x) + \frac{1}{\pi\hbar v_F \lambda} \int dx \Delta_i^2(x), \quad (1)$$

where

$$\Delta(x) = \Delta_e + \Delta_i(x) \exp(i\phi). \quad (2)$$

Here, Δ_e describes the intrinsic contribution to the energy gap, $\Delta_i(x)$ is the lattice distortion contribution to the energy gap, ϕ is the phase angle between the matrix elements describing the intrinsic contribution and the lattice distortion contribution to the energy gap, $\psi(x)$ is a two component spinor describing the electronic field, and σ_i are the Pauli spin matrices. The first term consists of two parts, the electronic kinetic energy and the electron-lattice interaction energy. The second term represents the elastic deformation energy of the polymer chain.

There are five material parameters in the BK model: Δ_e , ϕ , λ which describes the magnitude of the electron-phonon coupling and, therefore, the magnitude of the Peierls contribution to the energy gap; W is the undimerized bandwidth; and v_F is the Fermi velocity. It is convenient to define Δ_0 , the energy gap parameter of the homogeneous state for the corresponding degenerate $\Delta_e=0$ model, and Δ , the energy gap parameter of the homogeneous state for the nondegenerate model by

$$\Delta_0 = W \exp(-1/\lambda) \quad (3)$$

and

$$\Delta_e \cos(\phi) = \lambda [\bar{\Delta}^2 - \Delta_e^2 \sin^2(\phi)]^{1/2} \ln(\bar{\Delta}/\Delta_0). \quad (4)$$

The intrinsic contribution, Δ_e , breaks the degeneracy of the ground state of the BK model and admits charged excitations, which are polarons and bipolarons. Atomic relaxation around added charges (electrons and holes) occurs very rapidly and results in a lower total energy of the polymer. The energy per particle for two isolated polarons is greater than the energy per particle needed to create a bipolaron. Thus, there is additional binding of bipolarons relative to isolated polaron pairs. Upon transferring a high density of charge to the polymer, the lowest total energy configuration is a periodic bipolaron lattice.

In this section, we state the corrected self-consistency equations, which govern the formation of the bipolaron lattice in the nondegenerate continuum model.¹⁰ From the self-consistency equations, the effective single particle energy gap and the bipolaron upper and lower bands are computed at finite density. We also state the corrected energy per unit length for the bipolaron lattice, from which we calculate the chemical potential for the bipolaron lattice.

A. Self-consistency equations

The correct self-consistency equations [Eqs. (29) and (30) of Ref. 10] are

$$F(\beta, t) - \frac{\Delta_e \cos \phi}{\lambda} \frac{kE_2}{[-R(\Delta_1^2)]^{1/2}} = 0, \quad (5)$$

and

$$0 = (E_3^2 - \Delta_1^2)F(\beta, t) - (E_3^2 - E_2^2)\Pi(\beta, r'^2, t) + \frac{E_2 k}{2} \ln \left(\frac{\Delta_0^2}{E_3^2 + E_2^2 - E_1^2} \right), \quad (6)$$

where $F(\beta, t)$ and $\Pi(\beta, r'^2, t)$ are incomplete elliptic integrals of the first and third kind, respectively. Here $\Delta_1 = \Delta_e \sin(\phi)$, and $R(x)$ is defined in Ref. 10 and in the Appendix. The density of carriers per unit length in the bipolaron lattice (two carriers per bipolaron) is given by

$$n = \frac{k}{\hbar v_F K(r)}, \quad (7)$$

where $K(r)$ is the complete elliptic integral of the first kind. The values of E_1 , E_2 , and E_3 represent the lower and upper bipolaron band edges and half the effective single particle band gap, respectively. The elliptic modulus can be expressed in terms of these energies and is given by

$$r = \sqrt{\frac{E_3^2 - E_2^2}{E_3^2 - E_1^2}}, \quad (8)$$

and the conjugate modulus is

$$r' = \sqrt{1 - r^2}. \quad (9)$$

We also define

$$k = \sqrt{E_3^2 - E_1^2}, \quad (10)$$

$$\beta = \sin^{-1} \left(\frac{E_2}{E_3} \right), \quad (11)$$

and

$$t = \frac{E_3}{E_2} r'. \quad (12)$$

The energies E_1 , E_2 , and E_3 are computed from the self-consistency equations with the density given by Eq. (7). For PPV-like polymers, the physically relevant value for the phase angle is $\phi = 0$ (i.e., $\Delta_1 = 0$) and we restrict our attention to this case. It is convenient to define dimensionless variables $\eta = E_1/E_3$, $\zeta = E_2/E_3$, and $\sigma = E_3/\bar{\Delta}$. We define the scaled density \bar{n} by

$$n = \frac{\bar{\Delta}}{\hbar v_F} \bar{n}. \quad (13)$$

To numerically determine the energies, we consider the self-consistency equations and the scaled density to be functions of the two variables ζ and r' and obtain

$$\bar{n} = \frac{\sigma \sqrt{1 - \zeta^2}}{r K(r)}, \quad (14)$$

$$\sigma = \frac{\Delta_e}{\lambda \bar{\Delta}} \sqrt{\frac{1 - \zeta^2}{\zeta^2 - r'^2}} \frac{1}{F(\beta, t)}, \quad (15)$$

$$0 = F(\beta, t) - (1 - \zeta^2)\Pi(\beta, r'^2, t) + \frac{\zeta \sqrt{1 - \zeta^2}}{r} \ln \left(\frac{\Delta_0 r}{\sigma \bar{\Delta} \sqrt{1 - r'^2 \zeta^2}} \right). \quad (16)$$

To find the band energies E_1 , E_2 , and E_3 at a given density, we use Eq. (15) to eliminate σ and numerically solve Eq. (16) for ζ at fixed r' in the interval $0 \leq r' \leq 1$. This determines ζ as a function of r' . We then use Eq. (14) to determine r' for the given density. Once r' is determined, σ is calculated using Eq. (15), ζ is found using Eq. (16), and η is found from $\eta = \sqrt{\zeta^2 - r'^2}/r$.

B. Energy density and chemical potential

The correct bipolaron lattice energy per unit length [Eq. (33) of Ref. 10] is given by

$$W(n)/L = \frac{1}{\hbar v_F \pi} \left\{ \frac{F(\beta, t)}{E_2 k} [E_1^2 E_2^2 - \Delta_1^2 (E_3^2 + E_2^2 - E_1^2) + 2\Delta_1^2 k E(r) n \hbar v_F] + E_2 k E(\beta, t) + 2k E(r) n \hbar v_F \right. \\ \left. - \frac{2\Delta_e \cos \phi [-R(\Delta_1^2)]^{1/2}}{\lambda K(r)} \frac{E_3^2 - E_2^2}{E_3^2 - \Delta_1^2} \Pi \left(\frac{E_3^2 - E_2^2}{E_3^2 - \Delta_1^2}, r \right) + \frac{3}{2} \left(E_1^2 - E_2^2 - \frac{E_3^2}{3} \right) + (\bar{\Delta}^2 - 2\Delta_1^2) \ln \left(\frac{\bar{\Delta}}{\Delta_0} \right) + \frac{\bar{\Delta}^2}{2} \right\}, \quad (17)$$

where $E(\beta, t)$ is the incomplete elliptic integral of the second kind and $\Pi(\alpha, r)$ is the complete elliptic integral of the third kind. Intermediate steps of the derivation are given in the Appendix. Physically relevant parameters for PPV-like polymers correspond to $\phi=0$ and we restrict our attention to that case.

It is convenient to define a dimensionless energy per unit length w by

$$W(n)/L = \frac{\bar{\Delta}^2}{\hbar v_F} w. \quad (18)$$

The scaled energy per unit length can be expressed as a function of ζ and r' ,

$$w = \frac{\sigma^2}{\pi} \left[\frac{\zeta(\zeta^2 - r'^2)}{r\sqrt{1-\zeta^2}} F(\beta, t) + \frac{\zeta\sqrt{1-\zeta^2}}{r} E(\beta, t) + \frac{2(1-\zeta^2)E(r)}{r^2 K(r)} + \frac{3}{2} \left(\frac{\zeta^2 - r'^2}{r^2} - \zeta^2 - \frac{1}{3} \right) \right. \\ \left. - 2 \frac{\zeta(\zeta^2 - r'^2)}{r\sqrt{1-\zeta^2}} F(\beta, t) \frac{\Pi(1-\zeta^2, r)}{K(r)} \right] + \frac{1}{\pi} \left[\ln \left(\frac{\bar{\Delta}}{\Delta_0} \right) + \frac{1}{2} \right]. \quad (19)$$

The evaluation of the chemical potential is simplified by the elimination of singularities if we rewrite the complete elliptic integral of the third kind as $\Pi(1-\zeta^2, r)/K(r) = H(\zeta, r)$, where

$$H(\zeta, r') = 1 + \delta [E(\epsilon, r) - E(r)F(\epsilon, r)/K(r)]. \quad (20)$$

Here,

$$\delta = \frac{1}{\zeta} \sqrt{\frac{1-\zeta^2}{\zeta^2 - r'^2}}$$

and

$$\epsilon = \sin^{-1} \left(\frac{\sqrt{1-\zeta^2}}{r} \right).$$

The chemical potential is defined by

$$\mu = \frac{dW[n]/L}{dn} = \bar{\Delta} \frac{dw}{d\bar{n}} \quad (21)$$

and gives the energy per particle required to add a bipolaron to the polymer. The total derivative of the scaled energy density is evaluated from the ratio of the total differential of the scaled energy density,

$$dw = \frac{\partial w}{\partial \zeta} d\zeta + \frac{\partial w}{\partial r'} dr', \quad (22)$$

to the total differential of the scaled density,

$$d\bar{n} = \frac{\partial \bar{n}}{\partial \zeta} d\zeta + \frac{\partial \bar{n}}{\partial r'} dr'. \quad (23)$$

The chemical potential is given by

$$\frac{dw}{d\bar{n}} = \left(\frac{\partial w}{\partial \zeta} \frac{d\zeta}{dr'} + \frac{\partial w}{\partial r'} \right) \frac{dr'}{d\bar{n}}, \quad (24)$$

where the total derivative of ζ must be calculated.

The total derivative of ζ , with respect to r' , can be calculated from the self-consistency Eq. (16),

$$\frac{d\zeta}{dr'} = - \frac{\left(\frac{\partial G}{\partial r'} \right)_{\zeta}}{\left(\frac{\partial G}{\partial \zeta} \right)_{r'}}, \quad (25)$$

where G is the right hand side of Eq. (16). The partial derivatives can be calculated and combining the results, we obtain an analytic expression for the chemical potential. (See the Appendix for the analytic derivatives of the incomplete elliptic integral of the third kind.)

C. Numerical results for a bulk polymer

In the low density limit $r' \rightarrow 0$, the self-consistency equations reduce to a pair of equations, which determine the single bipolaron intragap level (E_0) and the energy gap parameter for the homogeneous state ($\bar{\Delta}$). The low density bipolaron formation energy per particle (E_b) can be found by taking the zero density limit of the chemical potential,

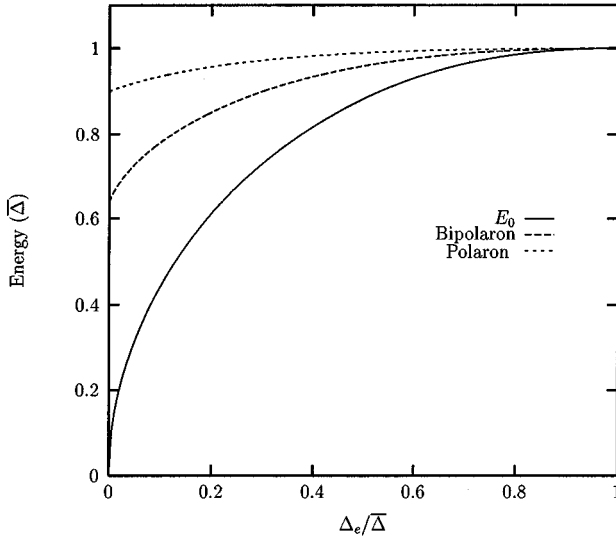


FIG. 1. Bipolaron formation energy per particle (dashed line), the bipolaron intragap level, (solid line) and the polaron formation energy (dotted line), as a function of $\Delta_e/\bar{\Delta}$.

$$E_b = \frac{\bar{\Delta}}{\pi} \left\{ 2\sqrt{1-\zeta_0^2} + \frac{\Delta_e}{\lambda\bar{\Delta}} \ln \left(\frac{1+\sqrt{1-\zeta_0^2}}{1-\sqrt{1-\zeta_0^2}} \right) \right\}, \quad (26)$$

where ζ_0 is the zero density value of ζ , which is equal to $E_0/\bar{\Delta}$. In the low density limit, the self-consistency equations reduce to the single bipolaron equations and the chemical potential to the single bipolaron formation energy per particle given by Onodera.⁹ There is an exact symmetry between electron and hole type excitations, so we only present results for electron type excitations.

In Fig. 1, we show the low density bipolaron intragap

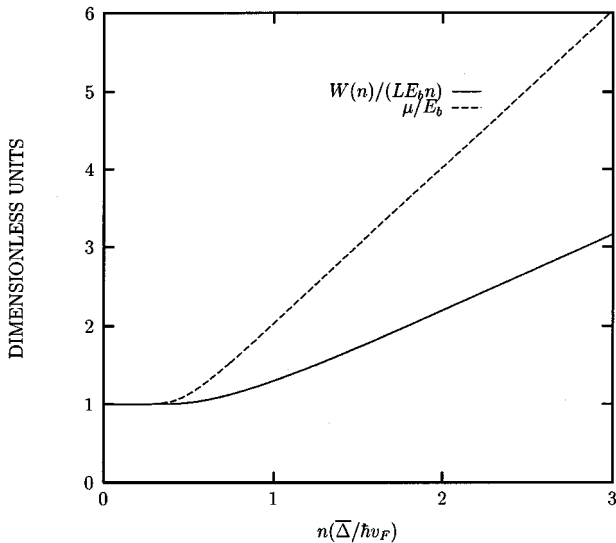


FIG. 2. Average energy per particle of the bipolaron lattice (dashed line) and chemical potential of the bipolaron lattice (solid line), in units of the zero density bipolaron formation energy per particle E_b , as a function of the scaled dimensionless chain bipolaron density.

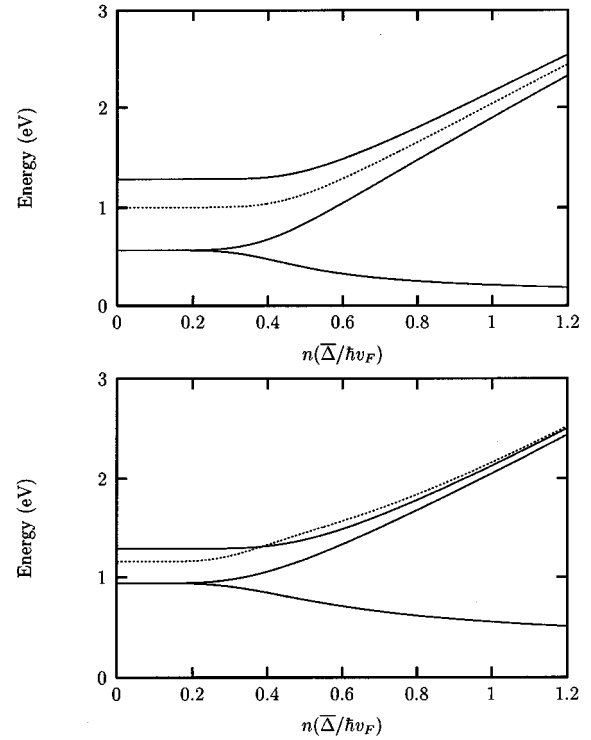


FIG. 3. The bipolaron energies E_1 , E_2 , and E_3 as a function of the scaled dimensionless chain bipolaron density. In the upper panel, the parameter values are $\Delta_e=0.1284$ eV, $\lambda=0.4385$, and $W=10$ eV. The dashed line is the chemical potential. In the lower panel, the parameter values are $\Delta_e=0.3849$ eV, $\lambda=0.3411$, and $W=10$ eV. For the upper panel $\Delta_e/\bar{\Delta}=0.1$ and the lower panel has $\Delta_e/\bar{\Delta}=0.3$. In both cases $\bar{\Delta}=1.284$ eV.

level (E_0), the bipolaron formation energy per particle (E_b) and the polaron formation energy,⁹ as a function of $\Delta_e/\bar{\Delta}$. The bandwidth W was fixed at 10 eV and λ and Δ_e were constrained so that $\bar{\Delta}$ was fixed at 1.284 eV. The ratio of $\Delta_e/\bar{\Delta}$ was varied. When $\Delta_e/\bar{\Delta}$ is equal to unity, the energy gap is determined entirely by the intrinsic splitting between bonding and antibonding levels, as in conventional semiconductors. When $\Delta_e/\bar{\Delta}$ is zero, the energy gap of the degenerate polymer is due entirely to the Peierls effect, as in trans-polyacetylene. The quantity $\Delta_e/\bar{\Delta}$ ranges from zero to unity and interpolates between a degenerate ground state polymer and a conventional one-dimensional semiconductor, respectively.

In Fig. 2, we show the average energy per particle (solid line) and the chemical potential (dashed line) of the bipolaron lattice, in units of E_b , as a function of density. Both are monotonically increasing functions of density. At low density ($\bar{n} \leq 1/3$), both the average energy per particle and the chemical potential are essentially equal to E_b . In Fig. 3, we show the energies E_1 , E_2 , and E_3 (solid lines) for two sets of input parameters, as a function of the normalized density. In Fig. 2 and the upper panel of Fig. 3, we have taken $W=10$ eV, $\Delta_e=0.1284$ eV, and $\lambda=0.4385$. In the lower panel of Fig. 3, we have taken $W=10$ eV, $\Delta_e=0.3849$ eV, and $\lambda=0.3411$. The Fermi velocity is 1.18×10^8 cm/sec in all calculations. The two cases in Fig. 3 correspond to $\Delta_e/\bar{\Delta}$

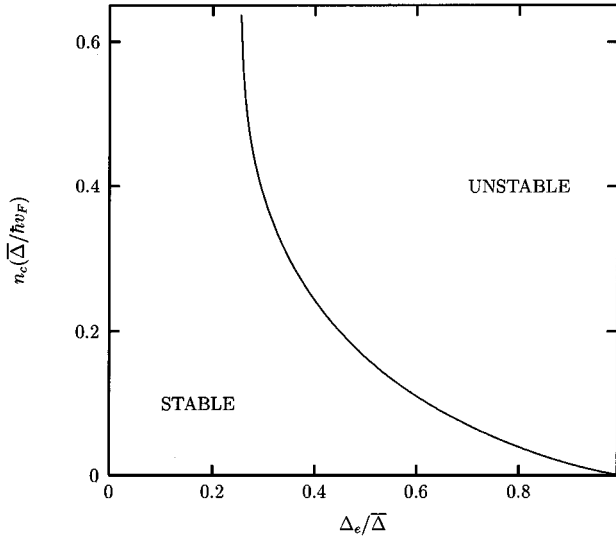


FIG. 4. The scaled critical density (i.e., the density where the chemical potential crosses E_3), as a function of $\Delta_e/\bar{\Delta}$. We have fixed $\bar{\Delta}=1.284$ eV; λ and Δ_e are varied to adjust $\Delta_e/\bar{\Delta}$.

equal to 0.1 and 0.3, respectively. Note that the single particle band gap and the bipolaron bandwidth increase with increasing density. As one approaches low density, the bipolaron bandwidth decreases rapidly to zero and approaches the single bipolaron intragap level $E_1=E_2=E_0$ and E_3 approaches the single particle gap parameter $\bar{\Delta}$. In the high density limit, we see that the behavior of the scaled energy parameters is given by $\zeta \rightarrow 1$, $\eta \rightarrow 0$ and σ increases monotonically with density.

In Fig. 3, the dotted lines are the computed chemical potential for the two sets of input parameters as a function of normalized density. In the upper panel, we note that $E_2 < \mu < E_3$, which indicates the stability of the bipolaron lattice for the complete density range considered. For $\Delta_e/\bar{\Delta}=0.3$, the chemical potential crosses E_3 at a finite critical density n_c . This indicates that the bipolaron lattice is unstable and further addition of charge into the system is not in the form of relaxed bipolarons. In Fig. 4, we show the critical density as a function of $\Delta_e/\bar{\Delta}$, where we have indicated the stable and unstable regions. Below the critical density n_c for fixed $\Delta_e/\bar{\Delta}$, the bipolaron lattice is stable and above the critical density it is unstable. We find that the bipolaron lattice is stable over the entire density range if $\Delta_e/\bar{\Delta}$ is less than about 0.25 for the present choice of the parameters. Increasing $\Delta_e/\bar{\Delta} \rightarrow 1$, the density range over which the bipolaron lattice is stable decreases and approaches zero. This is the limit of a conventional one-dimensional semiconductor, where the bipolaron is not a stable excitation.

III. METAL-POLYMER INTERFACE

The metal-polymer interface is described using the bulk electronic properties of the polymer computed from the non-degenerate continuum model. The metal is characterized by its work function. The polymer is characterized by the bipolaron chemical potential μ and the energies E_1 , E_2 , and

E_3 , which are specified as functions of density. The polymer is assumed to be in local equilibrium with the metal near the metal-polymer interface. The position of the metal Fermi level relative to the bipolaron chemical potential determines if charge transfer occurs at the interface. If the metal Fermi level is above the negative or below the positive zero density bipolaron chemical potential, then charge transfer to the polymer from the metal occurs and a bipolaron lattice is formed. This leaves a screening charge in the metal contact. There is no background doping, so the only charge in the polymer is from the metal contact.

The condition of local equilibrium allows the determination of the electrostatic potential throughout the polymer. The electrostatic boundary conditions are that the electrostatic potential in the metal is zero and the electric field vanishes deep in the polymer. We solve Poisson's equation for the electrostatic potential and the electric field in the polymer layer subject to these boundary conditions. Explicitly, we integrate

$$\frac{d^2\phi}{dx^2} = -\frac{4\pi\rho(\phi)}{\epsilon}, \quad (27)$$

where $\rho(\phi)$ is the charge density and ϵ is the dielectric constant of the bulk polymer. The charge density is given by

$$\rho(\phi) = -en(\phi)D, \quad (28)$$

where e is the magnitude of the electronic charge, $n(\phi)$ is the one-dimensional carrier density in the bipolaron lattice, and D is the two-dimensional density of polymer chains. For numerical calculations we take $\epsilon=3$ and the density of polymer chains determined experimentally for MEH-PPV,²⁰ $D=1.2 \times 10^{14}$ chains/cm².

The charge density within the polymer depends on the metal Fermi levels at the contacts and the electrostatic potential, which must be calculated self-consistently from Poisson's equation. The work function of the metal at the left contact μ_L fixes the chemical potential at the polymer interface, and therefore, determines the charge density in the polymer at the interface (by inverting the chemical potential expression for the density). The charge density within the polymer layer depends explicitly on the potential and is determined by inverting the electrochemical potential at each point in the polymer layer. The self-consistency is manifest, since Poisson's equation determines the electrostatic potential in the presence of the charged bipolarons, and the electrochemical potential depends on the electrostatic potential that determines the density of the bipolarons.

For the interface calculation, we fix W at 10 eV, $v_F=1.18 \times 10^8$ cm/sec, $\lambda=0.4385$, and $\Delta_e=0.1284$ eV. This gives a value for $\bar{\Delta}$ of 1.284 eV, a value for the polaron formation energy of $E_p=1.2$ eV, and a value for the bipolaron formation energy per particle $E_b=1.0$ eV. All of the energies are measured relative to the center of the zero density polymer gap.

In the upper panel of Fig. 5, we show $E_1(n(x))$, $E_2(n(x))$, $E_3(n(x))$, and $\mu(n(x))$ and in the lower panel of Fig. 5, we show $E_1(n(x))-e\phi(x)$, $E_2(n(x))-e\phi(x)$, $E_3(n(x))-e\phi(x)$, and $\mu(n(x))-e\phi(x)$ as a function of distance from the interface for a metal chemical potential of 1.3 eV. The polymer chains lie in the interface plane so that

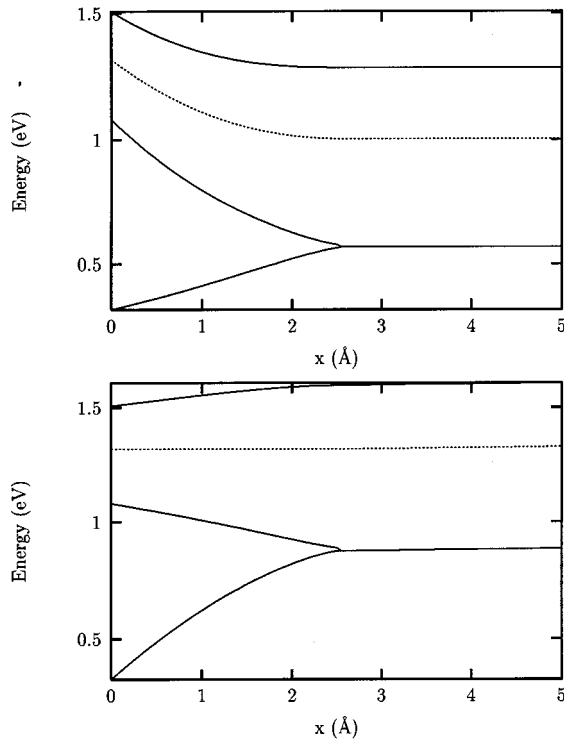


FIG. 5. E_1 , E_2 , E_3 , and $\mu(n(x))$ (dashed line) upper panel; and $E_1 - e\phi(x)$, $E_2 - e\phi(x)$, $E_3 - e\phi(x)$, and $\mu(n(x)) - e\phi(x)$ (dashed line) lower panel; as a function of distance from the interface.

the position axis in Fig. 5 corresponds to different chains lying at different distances from the interface. Because the metal chemical potential is larger than the bipolaron formation energy per particle, a high density of negative charge has been transferred from the metal to the polymer. This charge in the polymer is in the form of a one-dimensional bipolaron lattice in the polymer chains lying in the plane of the interface. There is a positive screening charge on the surface of the metal contact, which compensates the charge in the polymer. As seen in the upper panel of Fig. 5, $E_1(n(x))$, $E_2(n(x))$, $E_3(n(x))$, and $\mu(n(x))$ go to their zero density values far from the interface. As seen in the lower panel of Fig. 5, $\mu(n(x)) - e\phi(x)$ is constant as it must be at equilibrium.

The electric field near the interface is shown in the upper panel of Fig. 6 and the charge density near the interface is shown in the lower panel of Fig. 6 for various values of the metal work function larger than the bipolaron formation energy per particle ($E_b = 1.0$ eV). For realistic values of the density of polymer chains, an extremely large charge density is transferred into the polymer once the metal chemical potential exceeds the bipolaron formation energy. This large charge density results in extremely large electric fields, which cause a rapid spatial variation in $\rho(x)$. Because the distances involved are on the molecular scale, a continuum model cannot describe the spatial variation in detail. However, for most experimental situations, the details of the charge distribution on the molecular scale are not of interest. Essentially, there is a dipole layer at the metal-polymer interface in which one plate of the dipole layer is the charged

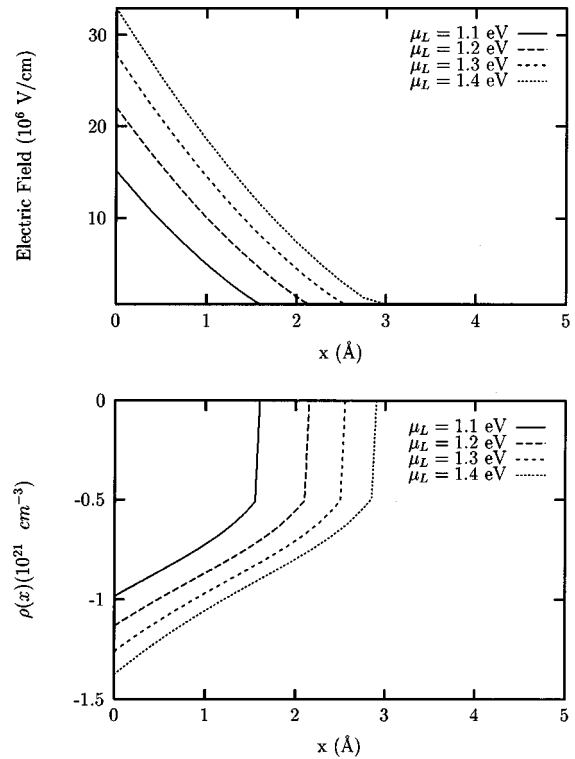


FIG. 6. The electric field (upper panel) and the charge density (lower panel) near the metal-polymer interface, as a function of distance for various values of the metal work function, $\mu_L = 1.1, 1.2, 1.3, 1.4$ eV, respectively.

bipolarons in the polymer and the other plate of the dipole layer is the screening charge in the metal. The essential point is that a very large charge transfer occurs once the metal Fermi level exceeds the bipolaron formation energy and this charge transfer causes a very large electric field over a short distance. This point is emphasized in Fig. 7, which shows the magnitude of the charge density (upper panel) and the electric field (lower panel) in the polymer at the interface as a function of the metal chemical potential. Both the charge density and electric field rise abruptly to very large values, as soon as the metal chemical potential exceeds the bipolaron formation energy. The calculations presented here are for zero temperature; at finite temperature activated charge transfer occurs when the metal chemical potential is below the bipolaron formation energy. Because the prefactor for the activated charge transfer is very large, it is significant for the metal chemical potential several $k_B T$ below the bipolaron formation energy.¹⁶

The spatial extent of the charged polymer region is very small and not directly accessible experimentally. The most interesting question about the charge transfer at the metal-polymer interface is how it affects the relative energy levels of states in the metal and states in the polymer beyond the narrow charged region. Specifically, we want to know the energy difference between the metal Fermi energy and the polaron formation energy in the polymer. (The polaron is the lowest energy singly charged transport state in the polymer.) This energy difference is the analog of the Schottky energy barrier at the interface between a metal and an inorganic semiconductor. When the metal Fermi level is below the bi-

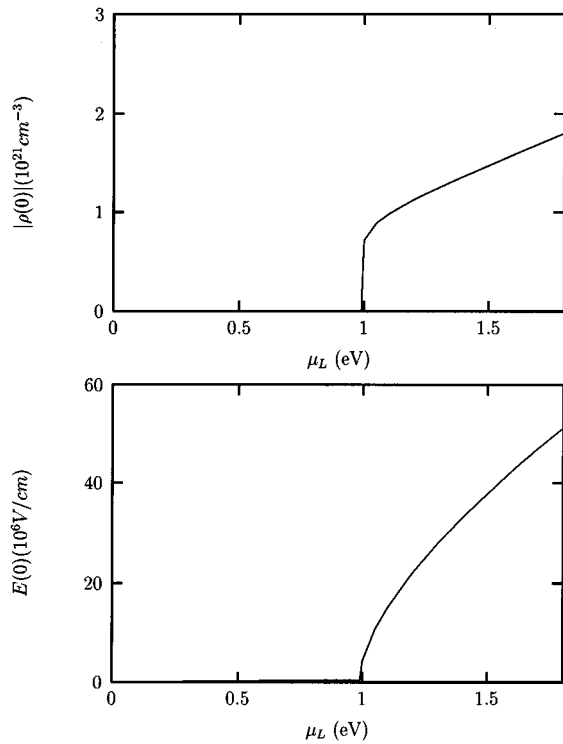


FIG. 7. The charge density (upper panel) and the electric field (lower panel) in the polymer at the interface, as a function of metal work function μ_L .

polaron formation energy per particle, there is no charge transfer and the effective Schottky barrier energy at the metal-polymer interface is just the energy difference between the polaron formation energy in the polymer and the metal Fermi energy. When the metal Fermi energy is above the bipolaron formation energy per particle, the change in electrostatic potential in the narrow charged region must be in-

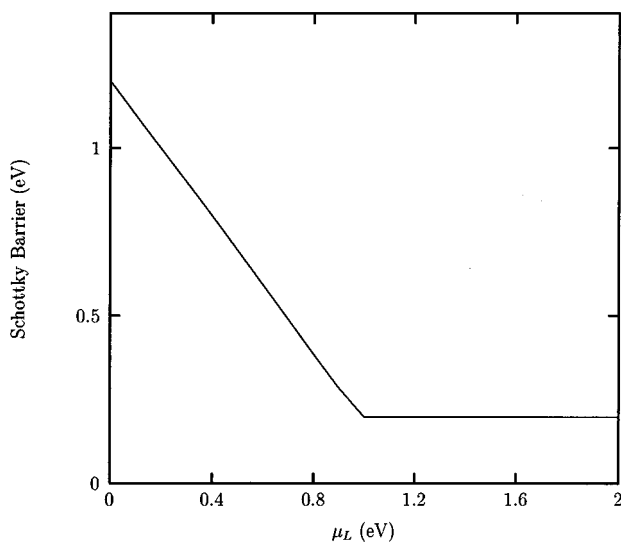


FIG. 8. The effective Schottky barrier energy, as a function of metal work function μ_L . The change in slope occurs at the bipolaron formation energy per particle.

cluded in the effective Schottky barrier energy. The effective Schottky barrier energy thus becomes $E_S = E_p - \mu_L - e\phi(x_c)$, where E_S is the effective Schottky barrier energy and $\phi(x_c)$ is the potential at the distance (x_c) at which the charge density has gone to zero. In Fig. 8, E_S is plotted as a function of the work function of the metal (μ_L) measured from the zero density gap center. At midgap ($\mu_L = 0$), the effective Schottky barrier is the polaron formation energy and E_S decreases linearly with increasing work function. When the metal work function coincides with the bipolaron formation energy, charge is transferred into the polymer layer and the Schottky barrier saturates. Further increase of the metal work function does not affect the barrier height, which is saturated at a value equal to the difference between the polaron and bipolaron formation energies of 0.2 eV for the present choice of parameters. The results in Fig. 8 are for zero temperature. At finite temperature, the abrupt shoulder that occurs in Fig. 8 is rounded and the saturation occurs several $k_B T$ lower in energy than the bipolaron formation energy per particle.¹⁶

A PLED device structure consists of a thin polymer film, typically 50–100 nm, sandwiched between two different metal contacts. One contact is a low work function metal and thus electron injecting and the other contact is a high work function metal and thus hole injecting. If a sufficiently large forward bias is applied to the device, electrons and holes are injected from the low and high work function contacts, respectively. The electrons and holes recombine in the polymer layer and emit light. From the description of the metal/polymer contact above, it is clear that the PLED structure can be divided into two contact regions, each of which is very thin compared to the total structure, and a central region. At zero bias, the electric field is essentially constant in the central region, because there is little or no charge in this region. At zero bias, the total change in electrostatic potential across the structure must equal the difference between the work functions of the two contacts. The electrostatic potential drop in a contact region is equal to the difference in energy between the work function and the bipolaron formation energy per particle, if charge transfer occurs or zero if it does not. Increasing (decreasing) the Fermi level of the electron (hole) injecting contact further above (below) the negative (positive) bipolaron formation energy per particle only increases the charge density transferred to the polymer and thus increases the region of rapid “band bending.” Therefore, the maximum potential drop across the central region of the structure at zero bias is given by the difference in the negative and positive bipolaron formation energies per particle. The maximum zero bias potential drop in the central region is reduced by several times $k_B T$ at finite temperature.

Applying an external bias to the device raises or lowers the Fermi level of one contact relative to the other. A reverse (forward) bias raises (lowers) the Fermi level of the high work function contact relative to the low work function contact. The magnitude of the electric fields, which result from an applied bias, are vastly smaller than those which occur in the contact regions and thus the structure, of the contact regions is not significantly affected by the applied bias. The increase in the potential drop across the structure which occurs at reverse bias (decrease in potential drop at forward bias), is entirely in the central region of the structure and

increases (decreases) the uniform electric field in the region. This behavior has been verified by detailed calculations.

IV. SUMMARY AND CONCLUSIONS

In this paper, we have presented an equilibrium model for the metal-polymer interface. The electronic properties of the polymer are determined within the nondegenerate continuum model of Brazovskii and Kirova. We presented the corrected bipolaron lattice solution to this model, both the self-consistency and the energy density equations. These equations are solved numerically for the electronic levels and are used to compute the bipolaron chemical potential for the bulk polymer. We found that the bipolaron lattice solution is stable below a critical bipolaron density, which is determined by the value of $\Delta_e/\bar{\Delta}$. For the parameters used, we found that the bipolaron lattice is stable at all densities if the intrinsic gap is less than approximately 25% of the single particle gap. If $\Delta_e/\bar{\Delta}$ is greater than about 25%, there is a critical density, above which the bipolaron lattice is unstable. This critical density decreases with increasing $\Delta_e/\bar{\Delta}$. The critical density goes to zero as $\Delta_e/\bar{\Delta}$ goes to unity.

The electronic energy levels and the bipolaron chemical potential completely characterize the electronic structure of the polymer within the nondegenerate continuum model. These results are used to examine the metal-polymer interface. Charge is transferred into the polymer from the metal contact if the Fermi energy of the metal is above the negative bipolaron formation energy per particle or below the positive bipolaron formation energy per particle. The charge transferred to the polymer is in the form of a bipolaron lattice. The spatial extent of the charge is limited to regions close to the interface and results in a narrow region of rapid “band bending.” The transferred charge pins the Fermi level of the metal at the value of the bipolaron formation energy. Since the effective Schottky barrier height at the interface is the energy difference between the Fermi level of the metal and the polaron formation energy after the region of rapid “band bending,” Fermi level pinning is seen to saturate the effective Schottky barrier height at the difference between the polaron and bipolaron formation energies.

A PLED structure consists of a thin polymer film between two different metal contacts. The structure can be divided into two contact regions, each of which is very thin compared to the total structure, and a central region. The total change in electrostatic potential across the structure must equal the difference in metal work functions, plus the applied bias. The structure of the contact regions is not affected by a moderate external bias. The electrostatic potential drop in a contact region is equal to the difference in the energy between the metal work function and the bipolaron formation energy per particle, if charge transfer occurs, or zero if it does not. The electric field is uniform (assuming no doping) in the central region and the magnitude of the field can be found by subtracting the potential drop in the contact regions from the total potential and dividing by the structure thickness. Capacitance-voltage measurements²⁰ show that MEH-PPV PLED structures have a central region, the thickness of which is bias independent under low injection conditions and approximately equal to the structure thickness, in which there is an essentially uniform electric field. Electroabsorp-

tion and internal photoemission measurements¹⁹ show that the effective Schottky barrier energies in MEH-PPV PLED structures scale directly with the metal work function, until a critical upper or lower value is reached, after which the effective Schottky barrier energy saturates and no longer depends on the metal work function. The observed critical values are such that they can be associated with negative and positive bipolaron formation energies per particle, respectively.¹⁹ Thus, these experimental results support the picture of the metal-polymer interface presented here. In the limit $\Delta_e \rightarrow 0$, our results reduce to the degenerate limit studied in Ref. 17.

In this work, the polymer chains were assumed to be aligned parallel to the metal/polymer interface, because that is the alignment found experimentally for soluble derivatives of PPV.¹⁸ As a result, the electric field is perpendicular to the polymer chain and the chain can be taken to be at a constant potential. The variation in the potential is between the polymer chains. If the chains were aligned perpendicular to the metal/polymer interface, the electric field would be parallel to the polymer chains. Because the field is very large near the interface, it might be expected to modify the internal structure of the bipolaron lattice. The main results presented here would not change dramatically, however, because they are based on very robust principles. When it is energetically favorable for charge to be transferred between the metal and intrinsic electronic states of the polymer, which occur at high density such as bipolarons, a large charge density is transferred. This transferred charge pins the Fermi energy at the point where charge transfer first becomes energetically favorable.

The polymer was described using the nondegenerate continuum model at zero temperature. In this model the bipolaron lattice is the stable state for excess charge. In a model which did not contain stable bipolarons, charge transfer would be in the form of polarons. The electrostatics of charge transfer to polarons would be similar to that for charge transfer to bipolarons. There is one significant difference between the two cases however. Charge injection under an applied external bias involves singly charged polaron states as the charge carrying species. The existence of bipolarons, which can pin the Fermi level at a lower energy than the polaron formation energy, leads to a minimum effective Schottky barrier for charge injection. This minimum effective Schottky barrier is the difference in the formation energy per particle of polarons and bipolarons.

ACKNOWLEDGMENT

We thank I. H. Campbell and A. R. Bishop for several stimulating discussions. This work was supported by the Los Alamos LDRD program.

APPENDIX: CALCULATIONAL DETAILS

The ground state elastic energy for the Hamiltonian Eq. (1) is given by

$$W_{\text{elastic}}^{\text{G.S.}} = \frac{L}{\lambda \hbar v_F \pi} [(\bar{\Delta}^2 - \Delta_1^2)^{1/2} - \Delta_e \cos \phi]^2,$$

and the ground state electronic energy is given by

$$W_{\text{electronic}}^{\text{G.S.}} = -\frac{L}{\hbar v_F \pi} \left[\left(E_{\Lambda}^2 - \frac{\bar{\Delta}^2}{2} \right) + \frac{\bar{\Delta}^2}{2} \ln \frac{4E_{\Lambda}^2}{\bar{\Delta}^2} \right],$$

where E_{Λ} is the energy corresponding to the upper momentum cutoff. The elastic energy of the bipolaron lattice is given by

$$W_{\text{elastic}}^{\text{B.L.}} = \frac{L}{\lambda \hbar v_F \pi} \left\{ \Delta_e^2 \cos^2 \phi + [E_3^2 + E_2^2 - E_1^2 - \Delta_1^2] \right. \\ \left. - 2kE(r)n\hbar v_F - \frac{2\Delta_e \cos \phi [-R(\Delta_1^2)]^{1/2}}{K(r)} \frac{4E_{\Lambda}^2}{E_3^2 - \Delta_1^2} \right. \\ \left. \times \Pi \left(\frac{E_3^2 - E_2^2}{E_3^2 - \Delta_1^2}, r \right) \right\}. \quad (\text{A1})$$

The electronic energy of the bipolaron lattice is given by

$$W_{\text{electronic}}^{\text{B.L.}} = \frac{L}{\hbar v_F \pi} \left\{ -E_{\Lambda}^2 + \frac{1}{2}(E_3^2 - E_2^2 + E_1^2) + E_2 k E(\beta, t) + \frac{1}{2}[E_1^2 - E_3^2 - E_2^2 + 2kE(r)n\hbar v_F] \ln \frac{4E_{\Lambda}^2}{\Delta_0^2} \right. \\ \left. + \frac{F(\beta, t)}{E_2 k} [E_1^2 E_2^2 - \Delta_1^2 (E_3^2 + E_2^2 - E_1^2) + 2\Delta_1^2 k E(r)n\hbar v_F] \right\}. \quad (\text{A2})$$

Combining these four terms and taking the energy cutoff to be $E_{\Lambda} = W \exp(1)/2$ gives the energy expression Eq. (17).

There is an ambiguity in the literature in the definition of the incomplete elliptic integral of the third kind. In the above, we have used the following definition:

$$\Pi(\phi, n, k) = \int_0^{\sin \phi} \frac{dx}{(1-nx^2)\sqrt{(1-x^2)(1-k^2x^2)}}. \quad (\text{A3})$$

The derivatives of $\Pi(\phi, n, k)$, with respect to k and n are, respectively, given by

$$\frac{\partial \Pi}{\partial k} = \frac{k}{n-k^2} \Pi(\phi, n, k) - \frac{k^2}{k'^2(n-k^2)} \left[\frac{E(\phi, k)}{k} \right. \\ \left. - \frac{k \sin \phi \cos \phi}{\sqrt{1-k^2 \sin^2 \phi}} \right], \quad (\text{A4})$$

$$\frac{\partial \Pi}{\partial n} = \frac{1}{2(1-n)(k^2-n)} \left[\frac{n \sin \phi \cos \phi \sqrt{1-k^2 \sin^2 \phi}}{1-n \sin^2 \phi} \right. \\ \left. + \left(1 - \frac{k^2}{n} \right) F(\phi, k) - E(\phi, k) + \left(n - 2(1+k^2) \right. \right. \\ \left. \left. + \frac{3k^2}{n} \right) \Pi(\phi, n, k) \right] - \frac{1}{n} \Pi(\phi, n, k). \quad (\text{A5})$$

We have used the following integral:

$$I = \int_a^u \frac{x^2 dx}{\sqrt{x(x-a)(x-b)(x-c)}} = \frac{2}{\sqrt{b(a-c)}} \left[b^2 F(\phi, k) \right. \\ \left. + (a^2 - b^2) \Pi(\phi, n, k) + n(a-b)^2 \frac{\partial \Pi}{\partial n} \right], \quad (\text{A6})$$

where $n = a/b$ and $u > a > b > c > 0$. In the derivation of the second self-consistency condition and the electronic energy

of the bipolaron lattice, the third incomplete elliptic integral for $n > 1$ can be converted to $N < 1$, using the formula

$$\Pi(\phi, n, k) = -\Pi(\phi, N, k) + F(\phi, k) + \frac{1}{2p_1} \ln \frac{\Delta(\phi) + p_1 \tan \phi}{\Delta(\phi) - p_1 \tan \phi}, \quad (\text{A7})$$

where $N = k^2/n$, $p_1 = [(n-1)(1-N)]^{1/2}$ and $\Delta(\phi) = (1-k^2 \sin^2 \phi)^{1/2}$.

The bipolaron lattice order parameter is defined by

$$\Delta_2(x) = \frac{\sqrt{-R(\gamma)} + \sqrt{-R(\Delta_1^2)}}{\gamma(x) - \Delta_1^2}, \quad (\text{A8})$$

where

$$\gamma(x) = E_3^2 - k^2 r^2 s n^2(kx, r)$$

and

$$R(\gamma) = (\gamma - E_1^2)(\gamma - E_2^2)(\gamma - E_3^2) \\ = -r^4 k^6 s n^2(kx, r) c n^2(kx, r) d n^2(kx, r). \quad (\text{A9})$$

Here, $sn(x, r)$, $cn(x, r)$, and $dn(x, r)$ are Jacobi elliptic functions²¹ and

$$\Delta_2^2(x) = E_3^2 - E_2^2 + E_1^2 - \Delta_1^2 - k^2 r^2 \{ c n^2(kx, r) \\ + c n^2[k(x+x_0), r] \}.$$

- ¹A. J. Heeger, S. Kivelson, J. R. Schrieffer, and W.-P. Su, *Rev. Mod. Phys.* **60**, 781 (1988).
- ²S. A. Brazovskii and N. N. Kirova, *Pis'ma Zh. Éksp. Teor. Fiz.* **33**, 6 (1981) [*JETP Lett.* **33**, 4 (1981)].
- ³J. H. Burroughes, D. D. C. Bradley, A. R. Brown, R. N. Marks, K. Mackay, R. H. Friend, P. L. Burn, and A. B. Holmes, *Nature (London)* **347**, 539 (1990).
- ⁴D. Braun and A. J. Heeger, *Appl. Phys. Lett.* **58**, 1982 (1991).
- ⁵G. Grem, G. Leditzky, B. Ulrich, and G. Leising, *Adv. Mater.* **4**, 36 (1992).
- ⁶P. L. Burn, A. B. Holmes, A. Kraft, D. D. C. Bradley, A. R. Brown, R. H. Friend, and R. W. Gymer, *Nature (London)* **356**, 47 (1992); M. Berggren, O. Inganäs, G. Gustafsson, J. Rasmusson, M. R. Andersson, T. Hjertberg, and O. Wennerstrom, *ibid.* **372**, 444 (1994).
- ⁷A. R. Brown, D. D. C. Bradley, J. H. Burroughes, R. H. Friend, N. C. Greenham, P. L. Burn, A. B. Holmes, and A. Kraft, *Appl. Phys. Lett.* **61**, 2793 (1992); D. Braun, A. J. Heeger, and H. Kromer, *J. Electron. Mater.* **20**, 945 (1991).
- ⁸G. Gustafsson, Y. Cao, G. M. Treacy, F. Klavetter, N. Colaneri, and A. J. Heeger, *Nature (London)* **357**, 477 (1992).
- ⁹Y. Onodera, *Phys. Rev. B* **30**, 775 (1984).
- ¹⁰S. A. Brazovskii, N. N. Kirova, and S. I. Matveenko, *Zh. Éksp. Teor. Fiz.* **86**, 743 (1984) [*Sov. Phys. JETP* **59**, 434 (1984)].
- ¹¹A. Saxena and J. D. Gunton, *Phys. Rev. B* **35**, 3914 (1987); **38**, 8459 (1988).
- ¹²A. Saxena and W. Cao, *Phys. Rev. B* **38**, 7664 (1988).
- ¹³H. W. Streitwolf, *Phys. Status Solidi B* **149**, K13 (1986); H. Puff and H. W. Streitwolf, *ibid.* **150**, 147 (1988); *Synth. Met.* **57**, 4431 (1993).
- ¹⁴M. Dinter, *Phys. Rev. B* **36**, 9628 (1987); **39**, 8423 (1989).
- ¹⁵S. A. Brazovskii and N. N. Kirova, *Self-Localization of Electrons and Periodic Superstructures in Quasi-1D Dielectrics*, Soviet Scientific Reviews (Harwood, New York, 1984), Vol. 5.
- ¹⁶P. S. Davids, A. Saxena, and D. L. Smith, *J. Appl. Phys.* **78**, 4244 (1995).
- ¹⁷S. A. Brazovskii and N. N. Kirova, *Synth. Met.* **56**, 2 (1993).
- ¹⁸D. McBranch, I. H. Campbell, D. L. Smith, and J. P. Ferraris, *Appl. Phys. Lett.* **66**, 1175 (1995).
- ¹⁹I. H. Campbell, T. W. Hagler, D. L. Smith, and J. P. Ferraris (unpublished).
- ²⁰I. H. Campbell, D. L. Smith, and J. P. Ferraris, *Appl. Phys. Lett.* **66**, 3030 (1995).
- ²¹I. S. Gradshteyn and I. M. Ryzhik, *Table of Integrals, Series, and Products* (Academic Press, New York, 1980).